Skeletal Radiol (2012) 41:1381–1390
DOI 10.1007/s00256-012-1358-9

SCIENTIFIC ARTICLE

Femoral morphology and epiphyseal growth plate changes of the hip during maturation: MR assessments in a 1-year follow-up on a cross-sectional asymptomatic cohort in the age range of 9–17 years

Karl-Philipp Kienle · Johannes Keck · Stefan Werlen · Young-Jo Kim · Klaus-Arno Siebenrock · Tallal Charles Mamisch

Received: 16 September 2011 / Revised: 26 December 2011 / Accepted: 5 January 2012 / Published online: 23 February 2012

Abstract
Objectives The goal of this prospective study was to characterize the morphology and physeal changes of the femoral head during maturation using MRI in a population-based group of asymptomatic volunteers.
Materials and methods Sixty-four pupils (127 hips) of 331 pupils from a primary and high school were asked to take part in this study and were willing to participate. 3T MRI of the hip was obtained at baseline and 1-year follow-up. With these images, we analyzed the femoral morphology and epiphyseal changes related to age, status of the physis, and location on the femur.
Results The radius of the femoral head and neck increased with age, as expected, ($p < 0.001$). The epiphyseal extension increased significantly with age ($p < 0.05$), but epiphyseal tilt and alpha angle showed no differences ($p > 0.05$). Building groups by using the epiphyseal status, we found that the epiphyseal extension had the highest changes in the "open" group and almost stopped in the "closed" group. The tilt angle did not change significantly ($p > 0.05$). Significant smaller alpha-angles were found in the "closed" group, however, these were in a normal range in all of them. Correlated to the position, the highest alpha-angle values were located in anterior-superior and superior-anterior position.
Conclusions Our data can be used as normative values, which can be compared to patients or cohorts with certain risk factors (e.g., professional athletes), this will offer the chance to detect and understand pathological changes.

Keywords Hip · Musculoskeletal abnormalities · Femoroacetabular impingement · Hip dysplasia · Pediatrics · Orthopedics

K.-P. Kienle · J. Keck · K.-A. Siebenrock · T. C. Mamisch
Department of Orthopedic Surgery, University of Bern, Bern, Switzerland

J. Keck
e-mail: keck.johannes@googlemail.com

K.-A. Siebenrock
e-mail: klaus.siebenrock@insel.ch

T. C. Mamisch
e-mail: mamisch@bwh.harvard.edu

S. Werlen
Department of Radiology, Sonnenhof Clinic, Bern, Switzerland
e-mail: stefanwerlen@sonnenhof.ch

Y.-J. Kim
Department of Orthopaedic Surgery, Children's Hospital, Harvard Medical School, Boston, MA, USA
e-mail: young-jo.kim@childrens.harvard.edu

K.-P. Kienle (✉)
Department of Orthopaedic Surgery, University of Bern, Inselspital, Bern, Schenkstraße 67, 91052 Erlangen, Germany
e-mail: philipp.kienle@gmail.com

Introduction

Structural hip abnormalities, such as hip dysplasia [1] and femoro-acetabular impingement (FAI) [2–4], have been implicated as an important cause of osteoarthrosis (OA) of the hip joint [5, 6], which seems to be the common final stage of mechanical distress of the hip. The underlying conditions that predispose to FAI include idiopathic pistol grip deformity [7], femoral neck fractures [8], slipped capital femoral

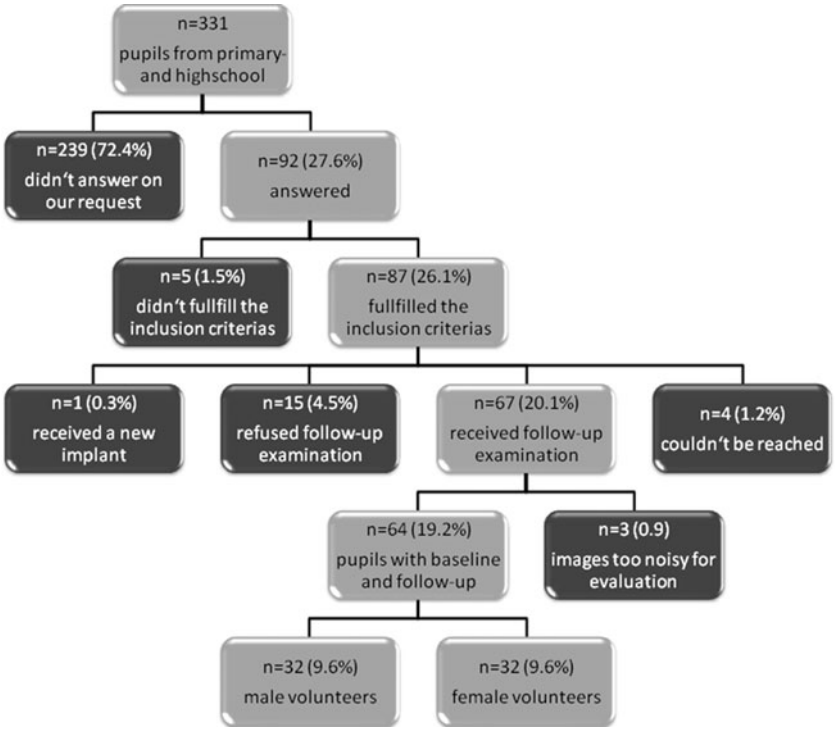

Fig. 1 Overview of the study population

epiphysis [9–12], acetabular retroversion [13], postoperative conditions [14], or other hip diseases e.g. aseptic bone necrosis (M. perthes) [15].

There are two different mechanical abnormalities of the hip leading to femoro-acetabular Impingement [16–19]. The "cam" impingement occurs due to a decrease in the femoral

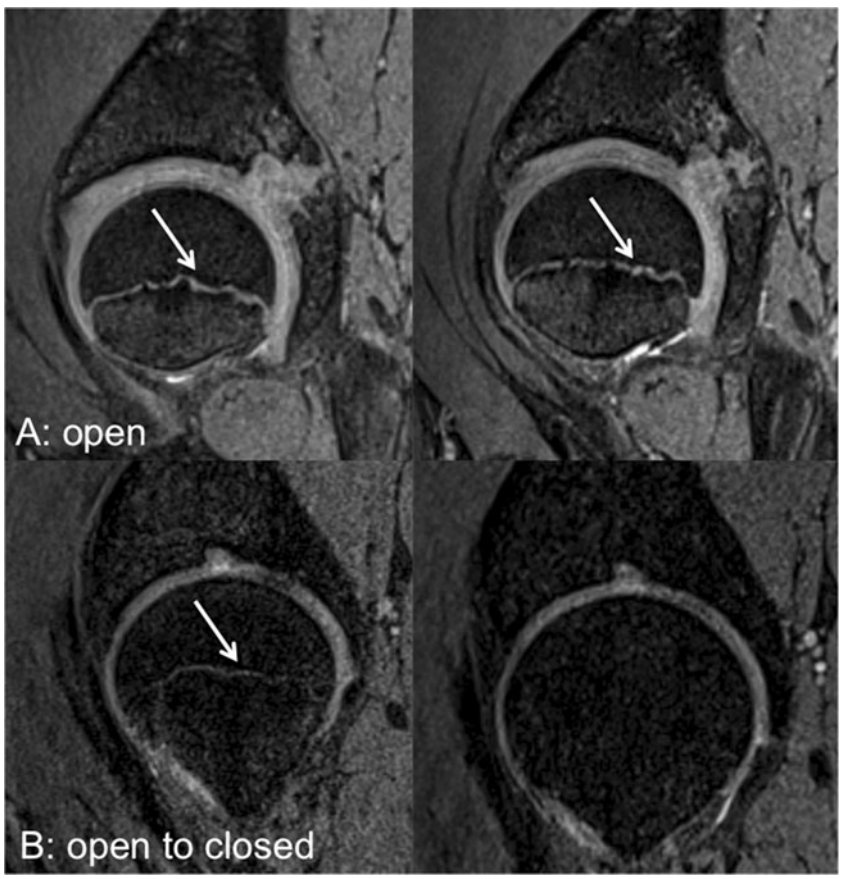

Fig. 2 Assessment of epiphyseal growth plate status between baseline and 1-year follow-up using 3D TrueFISP sequence. **a** A 10-year-old boy with open physis (*white arrows*) at both assessments. **b** A 13-year-old boy with open physis (*white arrows*) at baseline to closed physis at 1-year follow-up (*no physis visible*) ("open to closed")

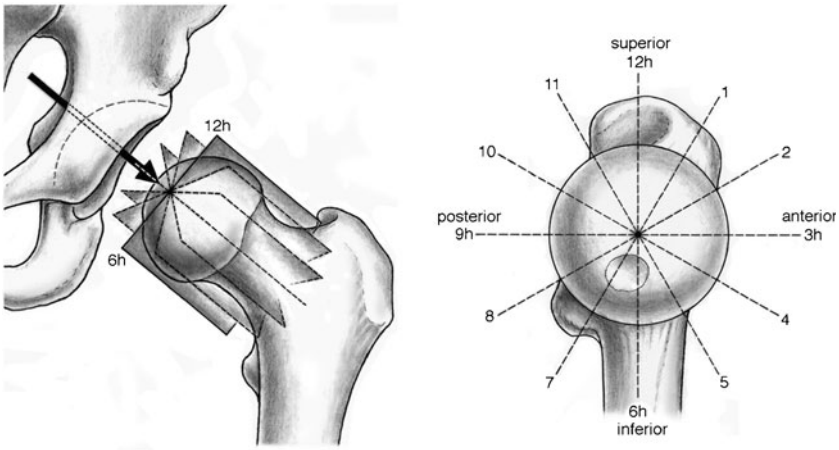

Fig. 3 **a** The radial MRI planes, which are perpendicular to the femoral head-neck axis, are defined on a sagittal oblique localizer. **b** The radial cuts are rotating clockwise at 30-degree intervals around the femoral head–neck axis from anterior to posterior

head-neck offset, mainly located in the anterior-superior part of the joint [9, 10, 20]. In these hips, the aspherical portion of the femoral head-neck junction enters the acetabulum, causing increased stress of the articular cartilage especially during hip flexion and internal rotation [9, 21].

"Pincer" impingement [16, 17, 21] has a pathomechanism depending on an increased acetabular overcoverage or retroversion. Hips with pincer impingement have an acetabulum that constrains the femoral head such that even with normal hip motion, contact between the acetabulum and femoral neck occurs, causing damage to the labrum, acetabular rim and articular cartilage. In most cases, it may be a mixture of these two types of mechanical abnormalities that leads to joint damage.

Due to the development of MR arthrography techniques with radial imaging around the femoral head and acetabular rim [22, 23], which gives the chance to evaluate the hip joint at different locations, different damage patterns like pistol grip deformity or acetabular retroversion have been defined more precisely and the degenerating factors like cam or pincer-impingement of the hip have been specified in much more detail. In addition to the increased image quality, several measurements, objectifying anatomical conditions of the hip, have been developed. For example, the alpha-angle described by Nötzli [20] and the head-neck-offset introduced by Eijer [24] are used to diagnose the degree of offset loss in patients with cam impingement. Wiberg's lateral center-edge-angle [25], acetabular depth [17] and the extrusion-index [26, 27] are used to determine acetabular coverage, e.g., in hip dysplasia or pincer impingement.

In the past, MR techniques have been used to reveal and evaluate the tibial and femoral physeal size, location, and signal intensity [28–30]. TrueFISP sequences seem to be a reliable tool for evaluating physeal structures.

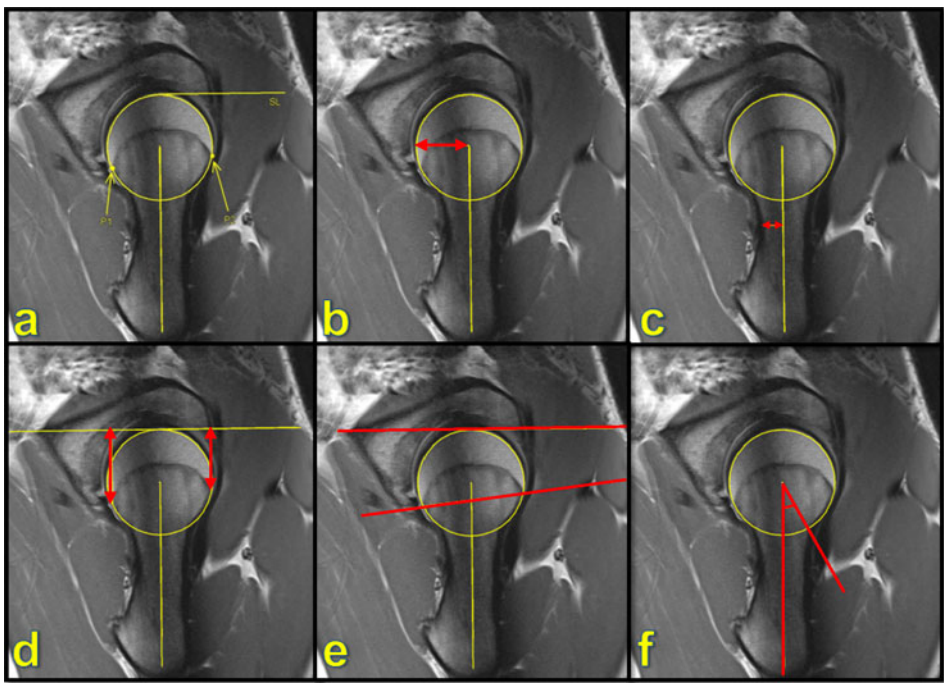

Fig. 4 Example of measurements to assess femoral morphology on the seven radial slices around the femoral neck: **a**. positioning of lateral and medial border of epiphyseal growth plate and the femoral neck axis for measurements **b**. head radius **c**. neck radius **d**. epiphyseal extension according to Siebenrock et al. [16] **e**. tilt angle according to Southwick et al. [40] **f**. alpha angle according to Nötzli et al. [25]

However, not much is known regarding the development of this characteristic hip deformity. For cam-type impingement, it appears that this deformity may be present during adolescence and its anatomic characteristics appear to be distinct from slipped capital femoral epiphysis [10].

To the best of our knowledge, careful characterization of hip development in adolescents using MRI has not yet been performed. The goal of this prospective study was to characterize the morphology of the femoral head and neck using MRI in a population-based group of asymptomatic volunteers. A secondary goal was to demonstrate the changes of the hip's epiphyseal growth plate during maturation in asymptomatic hips, for comparison with groups that may be at high risk for the development of FAI. We focused on the femoral head/neck morphology, using head and neck distance, tilt angle, epiphyseal extension, and alpha angle as indicators for pathological femoral development. These factors were assessed at baseline and 1-year follow-up.

Materials and methods

Population

The ethical commission of the university approved the study and written informed consent was obtained from both patients and parents.

For this prospective study, all pupils (n = 331) at a combined primary and high school (age range: 6–18 years) received an information letter asking for participation in a cross-sectional, longitudinal hip MRI study to assess the development of the hip.

Ninety-two pupils (28% out of all pupils) volunteered to participate in the study. Five (2%; 5/331) pupils were excluded based on exclusion criteria consisting of either hip pain, past or current hip disease (e.g., Legg-Calve-Perthes disease, hip dysplasia, slipped capital femoral epiphysis (SCFE) or others), previous hip surgery, or post-traumatic deformities. A total of

Table 1 Head and neck radius (mm) at baseline and 1-year follow-up measurements for different status of epiphyseal closure

		Growth plate grading		
		"Open"	"Open-closed"	"Closed"
Head radius (in mm)	Baseline	19.44 ± 2.11	21.04 ± 1.77	20.48 ± 1.51
	Follow-up	20.39 ± 2.30	21.40 ± 1.76	20.64 ± 1.49
	p value	0.02[a]	0.123	0.346
Neck radius (in mm)	Baseline	11.57 ± 2.11	12.17 ± 2.65	11.31 ± 2.08
	Follow-up	12.23 ± 2.24	12.43 ± 2.66	11.53 ± 2.00
	p value	0.01*	0.143	0.289

[a] Indicates statistical significance

Table 2 Epiphyseal extension (mm) at baseline and 1-year follow-up measurements for different status of epiphyseal closure

Epiphyseal-extension		Position					
Growth plate grading		Anterior	Anterior-superior	Superior-anterior	Superior	Superior-posterior	Posterior-superior	Posterior
"Open"	Baseline (in °)	1,937 ± 3.97	22.69 ± 3.50	25.78 ± 4.28	26.28 ± 3.91	26.40 ± 3.16	27.24 ± 3.88	26.10 ± 4.63
	Follow-up (in °)	20.49 ± 3.51	24.27 ± 3.79	27.47 ± 4.74	28.80 ± 4.19	28.18 ± 3.61	29.44 ± 4.22	28.44 ± 4.85
	p value	0.422	<0.001	<0.001	<0.001	<0.001	<0.001	<0.001
"Open-closed"	Baseline (in °)	22.98 ± 5.31	27.87 ± 4.02	30.98 ± 4.20	31.15 ± 4.36	30.25 ± 4.14	31.17 ± 3.85	28.99 ± 3.08
	Follow-up (in °)	23.25 ± 4.66	27.53 ± 4.88	31.05 ± 4.85	31.71 ± 4.46	30.87 ± 3.60	31.53 ± 4.25	29.00 ± 3.65
	p value	0.004	0.465	0.892	0.210	0.121	0.380	0.178
"Closed"	Baseline (in °)	22.89 ± 2.72	26.75 ± 3.08	29.36 ± 3.29	29.39 ± 3.24	29.14 ± 2.93	30.30 ± 2.62	29.55 ± 2.90
	Follow-up (in °)	22.92 ± 2.91	26.75 ± 2.97	29.51 ± 3.25	29.84 ± 3.11	29.17 ± 2.98	30.66 ± 2.22	29.89 ± 2.83
	p value	0.920	1	0.579	0.127	0.885	0.241	0.224

87 (26%; 87/331) pupils (mean age: 12.49 years; range: 6–17 years), 44 males (mean age: 12.50 years; range: 6–17 years) and 43 females (mean age: 12.48 years; range: 6–15 years) underwent baseline MRI and clinical examination. One patient was subsequently excluded from the study at the 1-year follow-up MRI examination because he had received a hip implant for traumatic destruction of the hip. Fifteen (4%; 15/331) participants refused the follow-up because of lack of interest and four (1%; 4/331) could not be reached.

In total, 67 (20%; 67/331) out of the initial 87 pupils underwent baseline and 1-year follow-up MRI. One volunteer refused an examination of his second hip joint because of claustrophobia, so, in total, 133 consecutive, corresponding MRI scans were obtained.

From these 133 hip MR assessments, six (1%; 3/331) series of images had to be excluded because the image quality was not diagnostic due to movement artefacts. Finally, 127 hips in 64 pupils (19%; 64/331), 32 females (mean age: 12.71 years; range: 7–15 years) and 32 males (mean age: 12.84; range: 7–17 years) were analyzed for this study. This is summarized in Fig. 1.

MR evaluation

MR examination was carried out using a 3 Tesla MR unit (MAGNETOM Trio, Siemens Medical Solutions, Erlangen, Germany), combined with a flexible surface coil (four-channel flex coil, Siemens Medical Solutions, Erlangen, Germany). We chose 3 T instead of 1.5 T to be able to guaranty a short length of examination to minimize movement artifacts occurring more often with extended length of examination, especially in young children. All volunteers were bedded in "feet first/supine" position, the lower extremities were fixed to minimize motion and to ensure a standard posture during examination. The coil was placed medially over the joint to have an optimal signal-to-noise ratio. The position was controlled by running a localizer of the whole pelvic and, if needed, changed.

For baseline and the 1-year follow-up-measurement, identical MRI-hip protocols were used. The examination included a sagittal three-dimensional (3D) T2-weighted SSFP (TrueFISP®) sequence (repetition time TR = 8.86 ms, echo time TE = 3.38 ms, flip-angle FA = 28°, field of view FOV = 120 cm, matrix = 256 × 256, acquisition time = 9.13 min) and a radial intermediate-weighted turbo spin-echo (TSE) sequence (TR = 1800 ms, TE = 12 ms, FA = 150°, FOV = 120 cm, matrix = 448 × 448, slice thickness 4 mm, acquired sections = 12, acquisition time = 1.55 min) to evaluate femoral head-neck junction, femoral head, and acetabulum perpendicular to the true plane of the acetabulum all around the axis of the femoral neck. Total scan time was about 13 min for each hip.

MR image evaluation

For further analysis, the data were transferred to a JiveX [dv] Viewer 4.1.1 workstation (Visus Technology Transfer GmbH, Bochum, Germany). State of the physis was rated by two observers (C. Mamisch with 3 years of experience in reading MR MSK images, P. Kienle with more than 10 years of experience in reading MR MSK images) using the

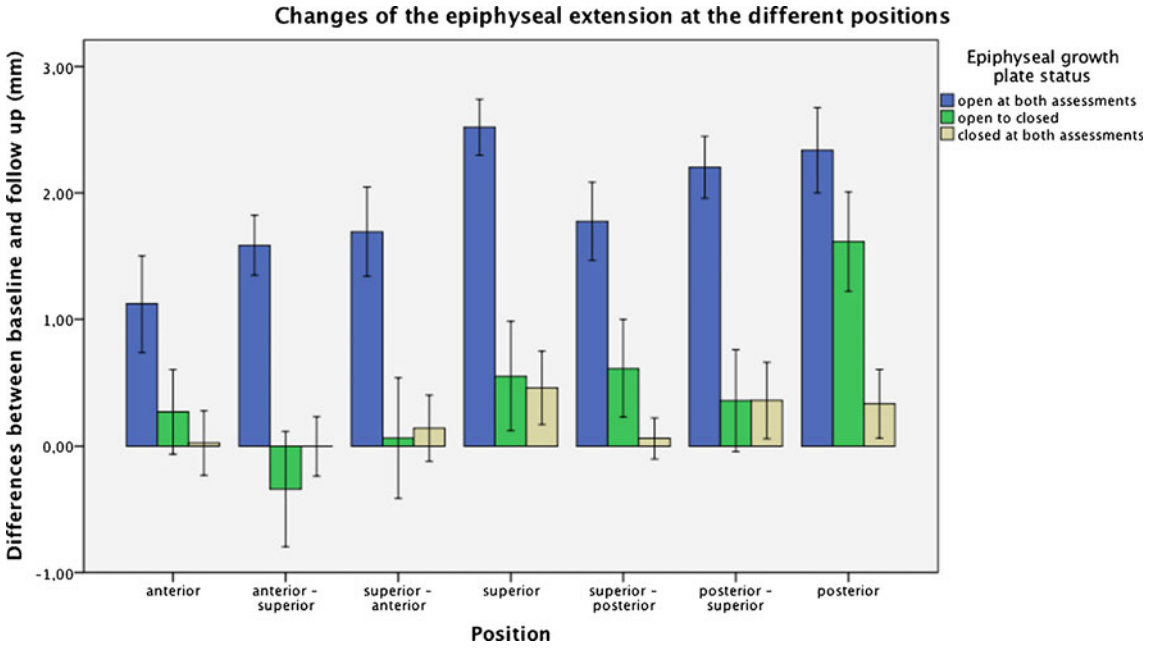

Fig. 5 Changes of the epiphyseal extension at the different positions: With open physis we found a clear trend with increased extension through each position. In the "open to closed" group, a different pattern with no changes/slight decrease in the anterior-superior and superior-anterior position is seen. The *asterisk* indicates significant differences between the first and second measurements

Table 3 Tilt angle (degrees) at baseline and 1 yr follow up measurements for different status of epiphyseal closure

tilt-angle		Position						
growth plate grading		anterior	anterior-superior	superior-anterior	superior	superior-posterior	posterior-superior	posterior
"open"	baseline (in °)	11.65±5.34	4.92±3.61	12.22±5.35	15.63±4.88	16.15±4.33	16.61±4.35	11.17±6.32
	follow up (in °)	12.63±4.90	4.67±3.17	11.98±5.38	16.55±5.04	16.27±3.88	17.10±3.95	12.12±6.07
	p-value	0.064	0.554	0.731	0.073	0.800	0.313	0.071
open-"closed"	baseline (in °)	8.98±4.98	6.71±4.67	17.20±4.95	20.65±3.89	18.63±4.33	18.42±4.87	8.98±4.98
	follow up (in °)	10.18±5.96	5.06±2.97	16.11±6.27	20.07±5.30	18.29±4.09	18.42±5.23	10.18±5.96
	p-value	0.134	0.102	0.219	0.396	0.642	0.999	0.134
"closed"	baseline (in °)	10.65±5.43	5.09±3.85	16.18±6.05	17.41±5.23	16.85±4.36	16.56±4.44	10.53±5.68
	follow up (in °)	11.16±4.44	3.75±2.89	14.74±5.56	17.57±4.54	16.05±3.13	16.54±4.87	10.64±5.61
	p-value	0.420	0.119	0.232	0.837	0.207	0.976	0.861

cartilage-sensitive 3D TrueFISP sequence. In three out 127 hips, the evaluation deferred and was revaluated in consensus by both observers. The capital femoral physis was evaluated and determined to be "open" or "closed" (Fig. 2). The capital physis was considered to be closed when the femoral head was represented by a homogeneous black signal without any intraosseous cartilage, which is typical for bones with closed physis. Hyperintense linear signal (indicating cartilage), demonstrated as a thin line through the entire head, is typical for femoral heads with open physis [31, 32] (Fig. 2). This classification was performed on baseline and 1-year follow-up scan.

The populations were classified by the status of the cartilaginous physis:

1) epiphysis cartilaginous (and therefore open [32]) at the first and the second examination (mean age: 11.61 years; range: 7–15 years);
2) epiphysis cartilaginous at the first and closed at the second examination (mean age: 13.38 years; range: 11–16 years);
3) epiphysis closed at the first and the second examination (mean age: 14.39 years; range: 12–17 years).

For all MR measurements the superior part of the hip joint was evaluated on seven radial slices rotating in 30° increments from anterior to superior to posterior position as described by Locher et al. [10, 22, 33] (Fig. 3).

For all measurements, a best-fitting circle was defined around the femoral head, thus the head center was determined. The axis of the femoral neck was determined by a line from the center of the femoral head oriented along the femoral neck axis by sense of proportion as described by Nötzli et al. [20]. Then, two points, which were located at the maximal range of the physis medial and lateral (P1 and P2) were determined and an orthogonal strait line (SL) on the axis of the femoral neck, being tangent to the circle we built around the femoral head, was drawn. These measurements are described in Fig. 4a. Based on this localization, the following measurements were performed:

(1) Head and neck radius: for the size of the head radius, we measured the radius of the idealized best-fitting circle around the femoral head (Fig. 4b) and for the neck radius, we took the smallest distance between the neck axis and the bony rim (Fig. 4c).

To describe the morphology of the physis the epiphyseal extension as described by Siebenrock et al. [10] and the tilt angle of the physis according to Southwick [34] who measured it on frog view radiographs was assed.

(2) Epiphyseal extension: Is defined as the distance from the orthogonal strait line to P2 (for anterior and

Table 4 Influence of epiphyseal growth-plate status

	Head-radius Highly significant ($p \leq 0.001$)	Neck-radius Highly significant ($p \leq 0.001$)	Tilt angle Significant ($p < 0.05$)	Epiphyseal extension Highly significant ($p \leq 0.001$)	Alpha angle Highly significant ($p \leq 0.001$)
Open	0.95±0.71 mm	0.56±1.32 mm	0.15 °±1.42°	1.89±1,29 mm	43.52°±7,17°
Open-closed	0.36±0.49 mm	0.26±1.35 mm	−0.81°±1.61°	0.44±0,96 mm	42.76°±9,02°
Closed	0.16±0.45 mm	0.22±1.32 mm	−0.46°±1.29°	−0.09±0.58 mm	39.38 ±9.93°

superior hemisphere) and to P1 (for posterior and inferior hemisphere) (Fig. 4d).

(3) Tilt angle: One side being represented by SL (orthogonal straight line), described above, the other side may be constructed by connecting P1 and P2. It is an open angle with no defined center (Fig. 4e).

In addition to assess femoral head-neck offset morphology we measured the alpha angle

(4) Alpha angle by Nötzli et al. [20]: this is the angle between the femoral neck axis and a line connecting the femoral head center with the point, where the bony shape of the femoral head leaves the previously created best-fitting circle around it (Fig. 4f).

Each measurement was done by two independent observers (P. Kienle with 3 years of experience in reading of MR MSK images, C. Mamisch with 10 years of experience in reading of MR MSK images) to assess the inter-observer variation. One observer (P. Kienle) repeated the measurements after 1 month to assess intra-observer agreement. Fur further analyses, mean values of one observer (P. Kienle) were used for each measurement.

Statistical analysis

The statistical analyses were done using PASW Statistics 17.0.2 (SPSS, Chicago, IL, USA). To compare the changes for the different time points and each measurement (baseline vs. 1-year follow-up) paired Student's *t* test was used. To assess the influence of ephiyseal growth plate status, one-way ANOVA with post-hoc analysis was used. The intra- and inter-observer was assessed using interclass-correlation (ICC) according to Strout and Fleiss [35] for quantitative variables.

Results

A total of 127 hips in 64 pupils ($n = 32$ male; $n = 32$ female) were analyzed. Sixty-five hips ($n = 33$, 11.61 years ± 1.85 years; range: 7–15 years) were classified into the group "open"; 26 hips ($n = 13$, 13.38 years ± 1.50 years; range: 11–16 years) into "open - closed" and 36 hips ($n = 18$, 14.39 years ± 1.04 years; range: 12–17 years) into the group "closed". None of the pupils had a different status of epiphyseal closure in the left and right hip. We have not yet examined the differences between sexes because we wanted to focus on the epiphyseal status, but we will do this in the next step.

Head and neck radius

If we looked at all studyparticipants the head radius increased statistically significant within the one year ($p > 0.05$) from 20.05 mm ± 2.01 mm to 20.67 mm ± 2.03 mm (difference 0.61 mm ± 0.71 mm), the neck radius, changed from 11.67 mm ± 2.25 mm to 12.08 mm ± 2.30 mm (difference 0.41 mm ± 1.33 mm) ($p > 0.05$).

The head radius differences between baseline and follow-up decreased significant ($p = 0.01$) from "open" (0.95 mm ± 0.71 mm) to "open - closed" (0.36 mm ± 0.49 mm) to "closed" (0.16 mm ± 0.45 mm). Similar results were found for the neck-radius differences between first and second measurement 0.56 mm ± 1.32 mm for the open group, 0.26 mm ± 1.35 mm for open-closed and 0.12 mm ± 1.32 mm for the closed one ($p = 0.01$).

There were no differences for femoral head or neck radius at the 7 positions around the femoral neck, neither in total nor depending on the subdivision of epiphyseal status. Values are summarized in Table 1.

Epiphyseal extension

Mean epiphyseal extension of all positions, regardless of subdivision by the state of the physis, increased significant ($p = 0.01$) from 26.70 mm ± 3.74 mm at baseline to 27.75 mm ± 3.56 mm at 1-year follow-up (difference 1.05 mm ± 1.40 mm).

The difference of epiphyseal extension changes decreased from "open" 1.89 mm ± 1.29 mm, to "open-closed" 0.44 mm ± 0.96 mm, to "closed" –0.09 mm ± 0.58 mm, where no significant ($p > 0.05$) changes could be observed. The influence of epiphyseal growth plate grading using ANOVA was significant ($p = 0.01$). This is summarized in Table 2.

By comparing the results for the different positions, no significant changes were seen for epiphyseal extension at the "open to closed" or "closed" group. In the "open" group,

Table 5 Alpha angle (degrees) at baseline and 1 yr follow up measurements for different status of epiphyseal closure

alpha-angle		Position						
growth plate grading		anterior	anterior-superior	superior-anterior	superior	superior-posterior	posterior-superior	posterior
"closed"	baseline (in °)	39.07±5.18	45.39±6.16	48.14±7.33	44.65±4.77	42.82±4.80	44.98±10.13	39.62±5.76
	follow up (in °)	39.34±4.99	45.44±5.71	49.27±8.22	44.48±5.58	42.48±5.12	45.01±10.84	39.77 ±5.91
	p-value	0.572	0.934	0.047	0.764	0.434	0.962	0.814
open-"closed"	baseline (in °)	39.09±7.67	49.43±8.70	47.74±7.54	41.98±6.23	40.41±6.41	43.65±12.05	37.03±6.74
	follow up (in °)	37.07±8.08	46.76±9.79	49.83±7.92	45.56±8.65	40.71±7.69	42.72±11.97	37.91±5.61
	p-value	0.047	0.005	0.309	0.001	0.798	0.441	0.475
"closed"	baseline (in °)	34.86±6.37	42.23±6.73	46.22±12.01	39.17±5.31	40.54±14.54	36.81±6.64	36.81±9.76
	follow up (in °)	34.13±6.90	40.87±6.36	47.43±11.60	40.80±5.27	40.58±15.07	38.82±5.43	37.28±9.01
	p-value	0.249	0.092	0.142	0.080	0.947	0.078	0.091

significant differences could be observed for the different positions. This is shown in Fig. 5.

Tilt angle

The mean tilt angle of all positions measured 13.15° ± 2.64° at the first date and 13.16° ± 2.51° at the second, with no statistical significant difference ($p = 0.273$).

The differences of tilt angle through all positions did not change significantly through the three groups of epiphyseal closure ($p = 0.128$).

When comparing the results for the different positions, no significant differences could be assessed in total or different groups of epiphyseal closure. These values are summarized in Tables 3 and 4

Alpha angle

The mean alpha angle of all positions did not change significantly from baseline (42.22° ± 8.58°) to 1-year follow-up scan (42.48° ± 8.79°) (difference 0.26° ± 4.77°) ($p = 0.568$).

Alpha angle changes through all positions not differed ($p = 0.584$) for epiphyseal growth plate status ("open": 0.17° ± 4.6°, "open to closed": 0.03° ± 5.7°, "closed": 0.33° ± 4.77°). The absolute values in the "open" group (43.52° ± 7.17) were significant ($p < 0.001$) higher than in the "closed" (39.38° ± 9.93°), however, only three out of 127 hips where in a pathological range with alpha angles higher than 55 degrees according to Nötzli et al. These three hips were classified as closed epiphyseal growth plate status (three out of 36 hips classified as closed, 8.3 %). The results are summarized in Table 4.

By comparing the results for the different positions, no differences were seen from anterior to posterior for "open" and "closed". For the "open to closed" group, from baseline to 1-year follow-up, the alpha angle was significant lower in anterior position (–1.9° ± 5.1°) and anterior-superior (–2.8° ± 4.6°), whereas significant higher values were found superior-anterior (2.32° ± 5.3°) and superior (3.6° ± 4.9°). The values are summarized in Table 5.

The ICC for inter-observer variation for head radius, neck radius, alpha-angle, tilt angle, and for epiphyseal extension was 0.918, 0.867, 0.705, 0.731, and 0.836, respectively.

The ICC for intra-observer assessment was 0.940 for head radius, 0.899 for neck radius, 0.839 for alpha angle, 0.878 for tilt angle, and 0.897 for epiphyseal extension.

Discussion

To the best of our knowledge, this is the first study to assess physiological changes of femoral morphology during

maturation using MRI. We found significant changes during maturation characterized by the epiphyseal growth plate status in a 1-year follow-up study.

The tilt angle of the physis did not change during maturation of asymptomatic hips, which means, because the extension of the physis, its movement towards the femoral neck, increases, that both ends of the physis have to moving similarly during physiological growth. Stuhlberg [7] and Goodman [4] thought of a subclinical slippage of the epiphysis leading to FAI. Normative values will be important in the future to determine if this slippage is responsible for anatomical pathologies promoting FAI.

In contrast, the epiphyseal extension globally increased until the physis was closed. After the closure, the movement onto the neck (extension) stops. The findings of changes of extension through growth are of importance, as epiphyseal extension is increased in patients with cam-type FAI morphology. Siebenrock et al. [10] described in 15 cases that the patients with FAI had significant higher extensions of the physis compared to a normal control group. This elongated epiphysis could only be found in the superior hemisphere of the joint, especially in the anterior-superior position.

Anatomical changes of a decreased head–neck offset were initially described by Stuhlberg [7] as a pistol-grip deformity and correlated to development of osteoarthrosis (OA). Nötzli et al. [20] quantified this deformity using the alpha angle and showed that these changes are seen in cam-type FAI. Our results suggest that in an asymptomatic cohort, the alpha angle remains relatively stable. There were some changes noted in the anterior-superior, superior-anterior, and superior regions in hips with open and open-closed physis. However, the direction of change was variable depending on the anatomic region, which means that during maturation, no general physiological changes to offset occur. With the closure of the physis, the alpha angle even slightly decreased in our cohort at anterior-superior position.

Our alpha angle measurements were in accordance with the normal values assessed by Nötzli [20] (42°, range: 33–48°), which supports no significant changes of normal alpha angles in asymptomatic cohorts during maturation. It is of interest that no pathological changes (alpha angle higher than 55°) were found in hips with open epiphyseal status in our cohort.

There are limitations in our study. We only had a 1-year follow-up examination, and the changes in maturation were therefore small, especially in the older pupils. However, we identified significant different patterns in development, which we will continue to follow. Another limitation is the interaction of acetabular and femoral changes, which were not assessed in this first analysis, as we focused only on femoral changes. These will be further assessed in ongoing analysis of this data.

Conclusions

In summary, we assessed the pattern of changes of femoral hip morphology in asymptomatic volunteers to create normative data that can ultimately be compared to patients or cohorts with certain risk factors for FAI (e.g., professional athletes). Future clinical use of this normative data depends on the MR classification of epiphyseal and femoral changes. These changes have to be differentiated into maturational (physiological) and pathological changes and into acquired versus congenital phenomena. This distribution will offer the chance to detect and understand pathological changes of the hip much earlier, so that preserving strategies of OA may be developed.

References

1. Murphy SB, Ganz R, Müller ME. The prognosis in untreated dysplasia of the hip. A study of radiographic factors that predict the outcome. J Bone Joint Surg Am. 1995;77(7):985–9.
2. Goodman DA, Feighan JE, Smith AD, Latimer B, Buly RL, Cooperman DR. Subclinical slipped capital femoral epiphysis. Relationship to osteoarthrosis of the hip. J Bone Joint Surg Am. 1997;79(10):1489–97. Erratum in: J Bone Joint Surg Am 1999 Apr;81(4):592. PubMed PMID: 9378734.
3. Beck M, Kalhor M, Leunig M, Ganz R. Hip morphology influences the pattern of damage to the acetabular cartilage: femoroacetabular impingement as a cause of early osteoarthritis of the hip. J Bone Joint Surg Br. 2005;87(7):1012–8. PubMed PMID: 15972923.
4. Ganz R, Leunig M, Leunig-Ganz K, Harris WH. The etiology of osteoarthritis of the hip: an integrated mechanical concept. Clin Orthop Relat Res. 2008;466(2):264–72. Epub 2008 Jan 10. Review. PubMed PMID: 18196405; PubMed Central PMCID: PMC2505145.
5. Harris WH. Etiology of osteoarthritis of the hip. Clin Orthop Relat Res. 1986;(213):20–33. PubMed PMID: 3780093.
6. Murray RO. The aetiology of primary osteoarthritis of the hip. Br J Radiol. 1965;38(455):810–24. PubMed PMID: 5842578.
7. Stulberg SD, Cordell LD, Harris WH. Unrecognized childhood hip disease: a major cause of idiopathic osteoarthrosis of the hip. The Hip Proceedings of the Third Meeting of The Hip Society. (Ed Amstutz HC). C.V. Mosby Company, Saint Louis 1975;212–28.
8. Eijer H, Myers SR, Ganz R. Anterior femoroacetabular impingement after femoral neck fractures. J Orthop Trauma. 2001;15(7):475–81. PubMed PMID: 11602829.
9. Ito K, Minka 2nd MA, Leunig M, Werlen S, Ganz R. Femoroacetabular impingement and the cam-effect. A MRI-based quantitative anatomical study of the femoralhead-neck offset. J Bone Joint Surg Br. 2001;83(2):171–6. PubMed PMID: 11284559.
10. Siebenrock KA, Wahab KH, Werlen S, Kalhor M, Leunig M, Ganz R. Abnormal extension of the femoral head epiphysis as a cause of cam impingement. Clin Orthop Relat Res. 2004;418:54–60. PubMed PMID: 15043093.
11. Mamisch TC, Kim YJ, Richolt JA, Millis MB, Kordelle J. Femoral morphology due to impingement influences the range of motion in slipped capital femoral epiphysis. Clin Orthop Relat Res. 2009;467(3):692–8. Epub 2008 Oct 22. PubMed PMID: 18941860; PubMed Central PMCID: PMC2635459.
12. Miese FR, Zilkens C, Holstein A, et al. MRI morphometry, cartilage damage and impaired function in the follow-up after slipped

capital femoral epiphysis. Skeletal Radiol. 2010;39(6):533–41. Epub 2010 Feb 24. PubMed PMID: 20177672.
13. Siebenrock KA, Schoeniger R, Ganz R. Anterior femoro-acetabular impingement due to acetabular retroversion. Treatment with periacetabular osteotomy. J Bone Joint Surg Am. 2003;85-A (2):278–86. PubMed PMID: 12571306.
14. Myers SR, Eijer H, Ganz R. Anterior femoroacetabular impingement after periacetabular osteotomy. Clin Orthop Relat Res. 1999;363:93–9. PubMed PMID: 10379309.
15. Eijer H, Berg RP, Haverkamp D, Pécasse GA. Hip deformity in symptomatic adult Perthes' disease. Acta Orthop Belg. 2006;72 (6):683–92. PubMed PMID: 17260605.
16. Kassarjian A, Brisson M, Palmer WE. Femoroacetabular impingement. Eur J Radiol. 2007;63(1):29–35. Epub 2007 May 7. Review. PubMed PMID: 17485190.
17. Pfirrmann CW, Mengiardi B, Dora C, Kalberer F, Zanetti M, Hodler J. Cam and pincer femoroacetabular impingement: characteristic MR arthrographic findings in 50 patients. Radiology. 2006;240(3):778–85. Epub 2006 Jul 20. Erratum in: Radiology. 2007 Aug;244(2):626. PubMed PMID: 16857978.
18. Kassarjian A, Belzile E. Femoroacetabular impingement: presentation, diagnosis, and management. Semin Musculoskelet Radiol. 2008;12(2):136–45. Review. PubMed PMID: 18509793.
19. Jaberi FM, Parvizi J. Hip pain in young adults: femoroacetabular impingement. J Arthroplasty. 2007;22(7 Suppl 3):37–42. Review. PubMed PMID: 17919591.
20. Nötzli HP, Wyss TF, Stoecklin CH, Schmid MR, Treiber K, Hodler J. The contour of the femoral head-neck junction as a predictor for the risk of anterior impingement. J Bone Joint Surg Br. 2002;84 (4):556–60. PubMed PMID: 12043778.
21. Ganz R, Parvizi J, Beck M, Leunig M, Nötzli H, Siebenrock KA. Femoroacetabular impingement: a cause for osteoarthritis of the hip. Clin Orthop Relat Res. 2003;(417):112–20. Review. PubMed PMID: 14646708.
22. Locher S, Werlen S, Leunig M, Ganz R. [MR-Arthrography with radial sequences for visualization of early hip pathology not visible on plain radiographs]. Z Orthop Ihre Grenzgeb. 2002;140(1):52–7. German. PubMed PMID: 11898065.
23. Werlen S, Leunig M, Ganz R. Magnetic resonance arthrography of the hip in femoroacetabular impingement: technique and findings operative techniques in orthopaedics. 2005;15(3):191–203.
24. Eijer H, Leunig M, Mahomed MN, Ganz R. Cross-table lateral radiograph for screening of anterior femoral head-neck offset in patients with femoro-acetabular impingement. Hip Int. 2001;11:37–41.
25. Wiberg G. Studies on dysplastic acetabulum and congenital subluxation of the hip joint with special reference to the complication of osteoarthritis. JAMA. 1940;115(1):81. doi:10.1001/jama.1940.02810270083038.
26. Herndon CH, Heyman CH. Legg-Perthes disease; a method for the measurement of the roentgenographic result. J Bone Joint Surg Am. 1950;32(A:4):767–78. PubMed PMID: 14784485.
27. Steppacher SD, Tannast M, Werlen S, Siebenrock KA. Femoral morphology differs between deficient and excessive acetabular coverage. Clin Orthop Relat Res. 2008;466(4):782–90. Epub 2008 Feb 21. PubMed PMID: 18288550; PubMed Central PMCID: PMC2504673.
28. Sasaki T, Ishibashi Y, Okamura Y, Toh S, Sasaki T. MRI evaluation of growth plate closure rate and pattern in the normal knee joint. J Knee Surg. 2002;15(2):72–6. PubMed PMID: 12013076.
29. Ecklund K, Jaramillo D. Patterns of premature physeal arrest: MR imaging of 111 children. AJR Am J Roentgenol. 2002;178(4):967–72. PubMed PMID: 11906884.
30. Craig JG, Cody DD, Van Holsbeeck M. The distal femoral and proximal tibial growth plates: MR imaging, three-dimensional modeling and estimation of area and volume. Skeletal Radiol. 2004;33(6):337–44. Epub 2004 Apr 3. PubMed PMID: 15064874.
31. Dvorak J, George J, Junge A, Hodler J. Age determination by magnetic resonance imaging of the wrist in adolescent male football players. Br J Sports Med. 2007;41(1):45–52. Epub 2006 Oct 4. PubMed PMID: 17021001; PubMed Central PMCID: PMC2465138.
32. Ulrich Welsch, Sobotta Lehrbuch Histologie: Zytologie, Histologie, Mikroskopische Anatomie.Seite 142–146 Verlag: Urban & Fischer Verlag; Auflage: 2., völlig überarb. A. (21. August 2006) Sprache: Deutsch ISBN-10: 3437444301.
33. Tanzer M, Noiseux N. Osseous abnormalities and early osteoarthritis: the role of hip impingement. Clin Orthop Relat Res. 2004; (429):170–7. Review. PubMed PMID: 15577483.
34. Southwick WO. Osteotomy through the lesser trochanter for slipped capital femoral epiphysis. J Bone Joint Surg Am. 1967;49(5):807–35. PubMed PMID: 6029256.
35. Strout PE, Fleiss JL. Intraclass Correlations: Uses in Assessing Rater Reliability. Psychology Bulletin. 1979;86:420–8.